Short-range correlations studies in collisions of polarized nuclei at Nuclotron-M

V.P. Ladygin[1,2,a], T. Uesaka[3], L.S. Azhgirey[1], Yu.V. Gurchin[1], A.Yu. Isupov[1], K. Itoh[4], M. Janek[1,5], J.-T. Karachuk[1,6], T. Kawabata[3], A.N. Khrenov[1], A.S. Kiselev[1], V.A. Kizka[1], A.B. Kurepin[7], A.K. Kurilkin[1,2], P.K. Kurilkin[1,2], V.A. Krasnov[1,7], N.B. Ladygina[1], D. Lipchinski[6], A.N. Livanov[1,7], Y. Maeda[8], A.I. Malakhov[1], G. Martinska[5], S. Nedev[9], S.M. Piyadin[1], E.B. Plekhanov[1], J. Popovichi[6], S. Rangelov[9], S.G. Reznikov[1], P.A. Rukoyatkin[1], S. Sakaguchi[10], H. Sakai[3,11], Y. Sasamoto[10], K. Sekiguchi[10], M.A. Shikhalev[1], K. Suda[10], A.A. Terekhin[1,12], J. Urban[5], T.A. Vasiliev[1,2], I.E. Vnukov[12], and H. Witala[13]

[1] Joint Institute for Nuclear Research, Dubna, Russia
[2] Moscow State Institute of Radio-engineering Electronics and Automation, Moscow, Russia
[3] Center for Nuclear Study, University of Tokyo, Tokyo, Japan
[4] Department of Physics, Saitama University, Urawa,Japan
[5] P.J.Šafarik University, Košice, Slovakia
[6] Advanced Research Institute for Electrical Engineering, Bucharest, Romania
[7] Institute for Nuclear Research, Moscow, Russia
[8] Kyushi University, Hakozaki, Japan
[9] University of Chemical Technology and Metallurgy, Sofia, Bulgaria
[10] RIKEN (the Institute for Physical and Chemical Research), Saitama, Japan
[11] University of Tokyo, Tokyo, Japan
[12] Belgorod State University, Belgorod, Russia
[13] Institute of Physics, Jagiellonian University, Krakow, Poland

Abstract. The status and prospects of 2-nucleon and 3-nucleon short range correlations (SRCs) studies at Nuclotron-M (JINR) are presented. This program is focused on the investigations of the spin part of SRCs with polarized deuteron beam from new high intensity polarized deuterons ion source which is under development at JINR. The wide experimental program on the systematic studies of the polarization effects in dp- elastic scattering, dp- nonmesonic breakup, $dd \rightarrow {}^3\text{He}n({}^3\text{H}p)$ and $d{}^3\text{He} \rightarrow p{}^4\text{He}$ reactions sensitive to SRCs using both internal and extracted beam at Nuclotron-M is presented.

1 Introduction

Short range correlations (SRCs) of nucleons in nuclei is the subject of intensive theoretical and experimental works during last years. Since SRCs have densities comparable to the density in the center of a nucleon which is about $\rho \sim 5\rho_0$ ($\rho_0 \approx 0.17$ fm^{-3}), they can be considered as the drops of cold dense nuclear matter [1]. These studies explore a new part of the phase diagram and very essential to understand the evolution of neutron stars.

The results obtained at BNL [2], SLAC [3] and JLAB [4,5] clearly demonstrate that: (i) more than 90% all nucleons with momenta $k \geq 300$ MeV/c belong to 2N SRC; (ii) probability for a given proton with momenta $300 \leq k \leq 600$ MeV/c to belong to pn correlation is ~18 times larger than for pp correlations; (iii) probability for a nucleon to have momentum ≥ 300 MeV/c in medium nuclei is ~25%; (iv) 3N SRC are present in nuclei with a significant probability [6]. However, still many open questions persist and

further investigations are required both from the experimental and theoretical sides. For instance, the experimental data on the spin structure of 2N (I=1) and 3N SRC are almost absent.

The main tools to study SRCs at hadronic facilities can be deuteron structure investigations at large internal momenta allowing to explore 2N SRC with $I = 0$; ^{3}He structure to understand the role of 2N SRC with $I = 1$ and 3N SRC; nuclei breakup $A(p, pp)X$, $A(p, pn)X$, $A(p, ppp)X$ etc. with the detection of few nucleons in the final state. The greate importance is the study of the spin effects in these reactions because the data on the SRCs spin structure are scarce. Nuclotron-M and NICA will allow to investigate the spin effects for multi-nucleon correlations in a wide energy range.

The model of 2N and 3N correlations at low and moderate energies (below pion threshold production) can be built from the boson-nucleon picture of strong interaction. During last several years a new generation of nucleon-nucleon potentials are built (Nijmegen, CD-Bonn, AV-18 etc.). These potentials reproduced the NN scattering data

ª e-mail: vladygin@jinr.ru

up to 350 MeV with very good accuracy. But these potentials cannot reproduce triton binding energy (underbinding is 0.8 MeV for CD-Bonn), deuteron-proton elastic scattering and breakup data. Incorporation of three nucleon forces (3NF), when the interaction depends on the quantum numbers of the all three nucleons, allows to reproduce triton binding energy and unpolarized deuteron-proton elastic scattering and breakup data (see [7] and references therein). The contribution of 3NF is found to be up to 30% in the vicinity of so called "cross section minimum" (Sagara discrepancy) for deuteron-proton elastic scattering at intermediate energies [8,9]. However, the use of different 3NF models in Faddeev calculations can not reproduce polarization data intensively accumulated during last decade at different facilities [8]–[14].

On the other hand, pd- elastic scattering cross section data obtained already at 250 MeV [11] cannot be reproduced by the Faddeev calculations with the inclusion of modern 3NF. The authors stated that the reason of this discrepancy can be neglecting by new type of short-range 3NF. These forces can be built within approaches beyond one-boson-exchange. For instance, in the dressed bag model [15] 3NF comes from the interaction between intermediate six-quark state dressed by σ-field and the third nucleon. The description of 2N and 3N correlations at the energies higher than several hundreds MeV/nucleon should be obtained within QCD [1].

The main goal of the DSS-project at Nuclotron-M is the systematic studies of the polarized deuteron-induced reactions at Nuclotron-M. The program includes two main directions.

– The measurements of the cross section, vector A_y and tensor A_{yy} and A_{xx} analyzing powers in dp- elastic scattering at large angles in cms in the energy range 0.3 – 2.0 GeV [16] and in dp- non-mesonic breakup at the energies below 500 MeV for different kinematic configurations of two final protons [17] at Internal Target Station (ITS) [18] at Nuclotron-M.

– The measurements of the cross section, tensor analyzing power T_{20} and spin correlation parameter $C_{y,y}$ in the d^3He $\rightarrow$ $p(0°)^4$He reaction [19]–[21] at the energies between 1000 and 2000 MeV using polarized ^{3}He target [22] and extracted polarized deuteron beam from new polarized ion source [23] at Nuclotron-M.

For these studies the development of the efficient polarimetry for deuteron and nucleon beams at intermediate and high energies at Nuclotron-M is necessary [16,24,25].

2 Measurements at Internal Target Station

The ITS setup is well suited for study of energy dependence of polarization observables for the deuteron-proton elastic scattering and deuteron breakup reaction with the detection of two protons at large scattering angles [16].

For these purposes the CH_2-target of 10 mkm thick is used for the measurements. The yield from carbon content of the CH_2-target is estimated in separate measurements

using carbon wire. The monitoring of the intensity is done from the detection of pp- quasielastic scattering at 90° in cms by the scintillation counters placed in the horizontal plane. The detection of the dp- elastic events is done by the coincidence measurements of the proton and deuteron. The detectors are placed in the horizontal plane only for the cross section measurements and in the both horizontal and vertical planes for the analyzing powers measurements. The selection of the dp- elastic events is done by the correlation of the energy losses in plastic scintillators for deuteron and proton and their time-of-flight difference. The interaction point for each event is reconstructed by the target position monitor [26].

The measurements of the deuteron analyzing powers in dp- elastic scattering have been performed at ITS using polarized beam from polarized ion source POLARIS [27] at the energies 880 and 2000 MeV [24,25]. The use of large amount of the scintillation counters allowed cover wide angular range. The measurement of the beam polarization has been performed at 270 MeV where the data on the tensor and vector analyzing powers based on the absolute calibration of the beam polarization exist [28].

2.1 dp-elastic scattering at 880 MeV

The results on the angular dependence of the vector A_y and tensor A_{yy} and A_{xx} obtained at 880 MeV are shown in Fig. 1 by the solid symbols. The solid, dashed and dash-dotted lines are the results of the Faddeev calculations [29] using CD-Bonn nucleon-nucleon potential [30], of the relativistic multiple scattering calculations [31] using CD-Bonn [30] deuteron wave function (DWF), and the optical potential calculation [32] with the dibaryon DWF [15], respectively. One can see that Faddeev and relativistic multiple scattering models give good description of the data except for A_{xx}.
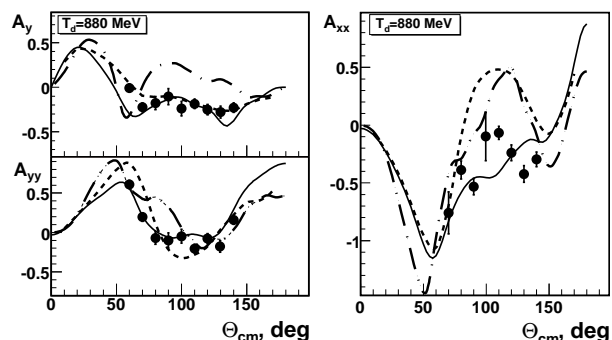

Fig. 1. Vector A_y, tensor A_{yy} and A_{xx} analyzing powers in dp-elastic scattering at 880 MeV [24,25]. The lines are the predictions of different models [29,31,32] (explained in the text).

On the other hand, Faddeev calculations [29] fail to reproduce the cross section at the angles larger than 90°, while relativistic multiple scattering calculations [33] give much better agreement with the data at the angles between

60° and 130°. The differential cross section of dp- elastic scattering at the deuteron kinetic energy of 880 MeV is presented in Fig. 2 as a function of the c.m. scattering angle. The full circles and squares are the data from refs.[34] and [35], respectively. The dashed and solid lines are the results of the calculations performed within relativistic multiple scattering model [33] without and with taking into account the rescattering, respectively.
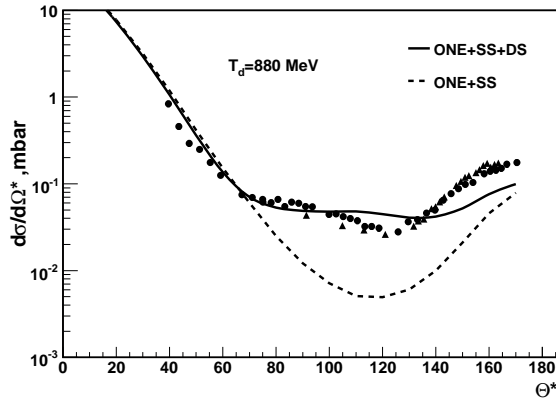
Fig. 2. The differential cross section of dp- elastic scattering at the deuteron kinetic energy of 880 MeV as a function of the c.m. scattering angle. The full circles and squares are the data from refs.[34,35], respectively. The dashed and solid lines are the results of the calculations perfomed within relativistic multiple scattering model [33] without and with taking into account the rescattering, respectively.

One can see a reasonable agreement between the calculations [33] and the experimental data [34,35] in the vicinity of the "cross section minimum". One of the reasons of some discrepancy in this region can be 3N SRCs, which are not included in the calculations. These SRCs can be responsible for the deviation between the calculations [31] and data on the analyzing powers [24,25] also.

The shape of the differential cross section for the dp-elastic scattering at 500 MeV obtained at ITS at Nuclotron [16] is in good agreement with the RCNP data [11]. It is planned to perform the systematic measurements of the dp- elastic scattering cross section and analyzing powers at the energies 200-500 MeV/nucleon at ITS.

## 2.2 Energy dependence of the dp- elastic scattering analyzing powers

The dependences of the tensor A_{yy} and vector A_y analyzing powers in dp- elastic scattering obtained at the fixed angles of 60°, 70°, 80° and 90° in the c.m. as a function of transverse momentum p_T are shown in Fig. 3 and in Fig. 4, respectively. The open and solid symbols represent the data obtained at RIKEN, Saclay, ANL [8–10,36–38] and at Nuclotron [24,25], respectively.

The values of A_{yy} are positive at small p_T and change the sign at $p_T \sim 600$–650 MeV/c as in the case of deuteron
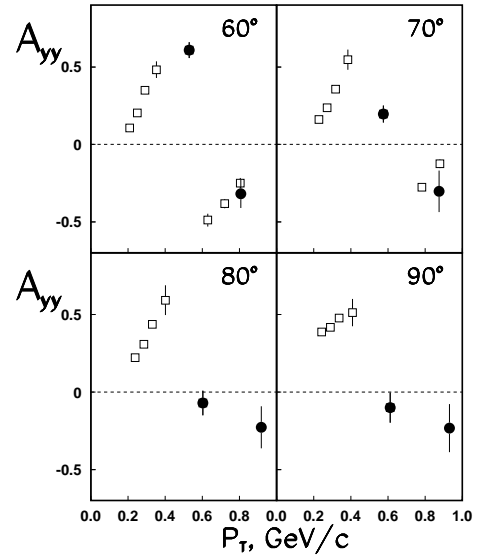
Fig. 3. Tensor A_{yy} analyzing power in dp- elastic scattering obtained at the fixed angles of 60°, 70°, 80° and 90° in the c.m. as a function of transverse momentum p_T. The open and solid symbols are the data obtained at RIKEN, Saclay, ANL [8–10,36–38] and at Nuclotron [24,25], respectively.

inclusive breakup [39]. The negative sign of A_{yy} is observed at large p_T. It would be interesting to extend the range of the measurements to larger p_T, where the manifestation of non-nucleonic degrees of freedom is expected.
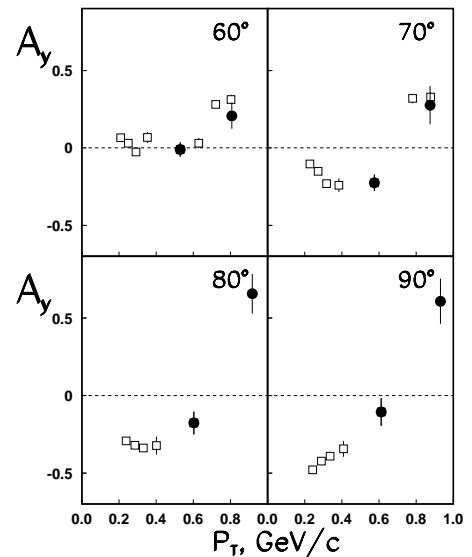

Fig. 4. Vector A_y analyzing power in dp- elastic scattering obtained at the fixed angles of 60°, 70°, 80° and 90° in the c.m. as a function of transverse momentum p_T. The symbols are the same as in Fig. 3.

The change of the sign is also observed for the vector A_y analyzing power values at p_T ~600–700 MeV/c at large angles in the c.m. A_y has small negative values at low p_T, but it achieves large positive values at p_T higher ~700 MeV/c. It should be noted that large positive values of the single spin asymmetry is observed in pp- elastic scattering at high energies and large p_T (so called Krisheffect [40]). For dp- elastic scattering such effect is observed at rather low p_T. Further precise measurements are required to understand the reason of such behavior.

The study of the energy dependence of the dp- elastic scattering analyzing powers at large p_T is one of the tools to study spin effects in cold dense matter.

2.3 dp- nonmesonic breakup

The study of dp- breakup reaction in different kinematic configurations gives an opportunity to select the regions of phase space where the observables are sensitive mostly to 2NF or 3NF. While the breakup data at the energies of 65-135 MeV/nucleon [41–44] are quite systematic, the lack of the experimental information exists at higher energies. The predictions of the polarization observables and cross section for dp- non-mesonic breakup at 400 MeV for different kinematic configurations of the final protons are given in ref. [45,46]. The observables for some kinematic configurations demonstrate strong sensitivity to the contribution of 3NF.
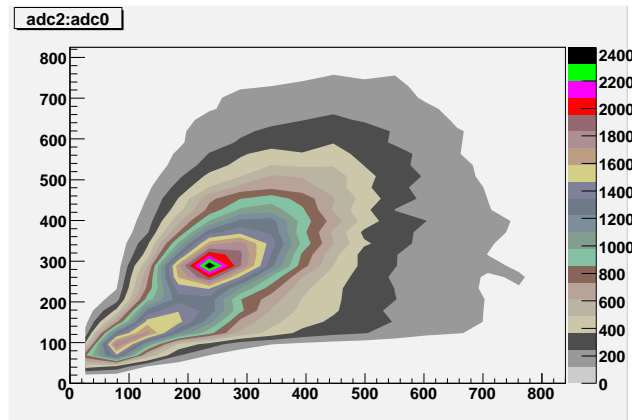
Fig. 5. The correlation of the energy depositions in two E counters obtained at ITS with 2.3 GeV deuteron beam [17].

The dp- non-mesonic breakup reaction will be investigated at ITS at Nuclotron using ΔE-E techniques for the detection of two final protons. Monte-Carlo simulation shown the feasibility of such techniques for the energies $T_d \leq 500$ MeV [47]. Each detector consists of two scintillation counters: the first and the second ones are with 1 cm and 20 cm scintillators in length, respectively. The diameter of the E-counter scintillator is 10 cm. The use 8-10 ΔE-E detectors simultaneously will allow to measure the observables for many kinematic configurations. The results on the amplitudes signals correlation for two

E detectors obtained during beam test run in June 2008 at ITS using 2.3 GeV deuterons [17] are presented in Fig. 5. The measurements will be performed at the energies below 250 MeV/nucleon at the same time with the measurements of dp- elastic scattering. However, additional time will be required to estimate reliably contribution from the carbon content of CH_2 target.

The measurements of the cross sections of dp- elastic scattering and dp- nonmesonic breakup can be done with the current unpolarized ion source. The realization of the spin program at ITS can be started with the intensity of the POLARIS ($\sim 2 \cdot 10^8$ ppp) [27] maintained from the present value by the recovering of the intensity losses during the injection into Nuclotron ring. The energy scan of the dp-elastic scattering observables can be done with new high intensity PIS [23].

3 Measurements at extracted beam

The goal of the ^{3}He(d, p)^{4}He reaction study at Nuclotron-M is to understand the reasons of the long staying puzzle, namely, the behavior of the tensor analyzing power T_{20} in dp- backward elastic scattering [48,49]. While t_{20} data in ed- elastic scattering obtained at JLAB [50] and T_{20} data in dp- inclusive breakup [51,52] can be explained by using the conventional deuteron structure functions and additional to the Born approximation mechanisms, the T_{20} in dp- backward elastic scattering demonstrate unexplained strange structure at the internal momentum k ~0.3–0.5 GeV/c in the vicinity of the D- wave dominance in the deuteron.

The experiments performed at RIKEN at the energies below 270 MeV have shown that the polarization correlation coefficient

$$C_{//} = 1 - \frac{1}{2\sqrt{2}}T_{20} + \frac{3}{2}C_{y,y} \qquad (1)$$

for the ^{3}He(d, p)^{4}He reaction may be a unique probe to the D-state admixture in deuteron [19]. The usefulness of this observable to investigate the D-state admixture is attributed to the strong spin-selectivity in neutron capture process by ^{3}He nucleus, i.e., spins of transferred neutron and ^{3}He must be anti-parallel to each other in order to form ^{4}He in the final state. In the Born approximation, the expression for $C_{//}$ is proportional to the D-state fraction in deuteron as

$$C_{//} = \frac{9}{4}\frac{w^2}{u^2 + w^2}, \qquad (2)$$

where u and w are the S- and D-state wave functions of deuteron in momentum space. This is a marked contrast to T_{20} and κ_0 for dp backward elastic scattering which include S- and D-state interference term (uw-term) together with a w^2-term. It is thus expected that $C_{//}$ may be a candidate to provide an information on the deuteron structure complementary to those from T_{20} and κ_0 obtained in dp-backward elastic scattering [48].
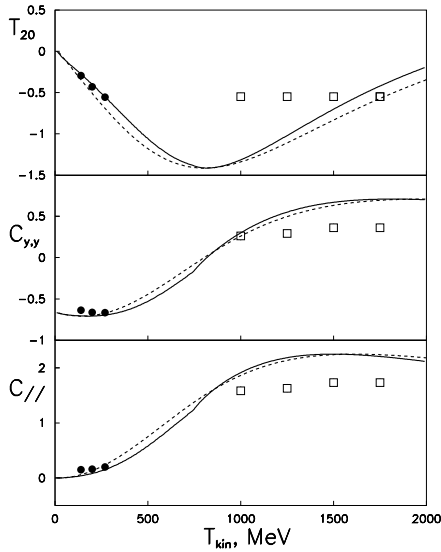
Fig. 6. Tensor analyzing power T_{20}, spin correlation $C_{y,y}$ and polarization correlation coefficient $C_{//}$ for the ${}^3\text{He}(d, p)^4\text{He}$ reaction. The dashed and solid lines represent one-nucleon exchange calculations without [20] and taking into account the Fermi motion in the target nucleus, respectively. The full symbols are the data obtained at RIKEN [21]. The open squares show the expected precision for the data at Nuclotron-M.

Tensor analyzing power T_{20}, spin correlation $C_{y,y}$ and polarization correlation coefficient $C_{//}$ for the ${}^3\text{He}(d, p)^4\text{He}$ reaction are shown in Fig. 6. Solid lines in the figures represent calculations based on an impulse approximation proposed in Ref. [20]. In the calculation, the Fermi motion in the target nucleus is taken into account [21]. The full symbols are the data obtained at RIKEN [21]. The open squares show the expected precision for the data at Nuclotron-M.

The main goal of the experiment is to obtain the data on $C_{//}$ in the energy region of 1.0–1.75 GeV, where the contribution from the deuteron D-state is expected to reach a maximum in one-nucleon exchange approximation, to obtain new information on the strange structure observed in the behavior of T_{20} in the dp- backward elastic scattering and to realize experiment on the full determination of the matrix element of the ${}^3\text{He}(d, p)^4\text{He}$ reaction in the model independent way. These data will help us also to understand the short-range spin structure of deuteron and effects of non-nucleonic degrees of freedom. For these purposes polarized deuteron beam from new PIS [23] and polarized ${}^3\text{He}$ target developed at CNS of Tokyo University [22] and modified for present experiment at Nuclotron-M will be used.

The data on the analyzing powers in $d(d, {}^3\text{He})n$ and $d(d, {}^3\text{H})p$ obtained at 270 and 200 MeV [53] are shown in Fig. 7. The curves are the calculation within one-nucleon-exchange approximation using standard deuteron and ${}^3\text{He}({}^3\text{H})$ wave functions [54]. The data demonstrate the sensitivity to the D/S waves ratio in these light nu-

clei at short internucleonic distances. However, the calculations[54] fail to reproduce the data. The reason of the discrepancy can be in the non-adequateness of the 3N-bound state spin structure and/or more complicated reaction mechanism. The multiple scattering calculations are in progress now [33].
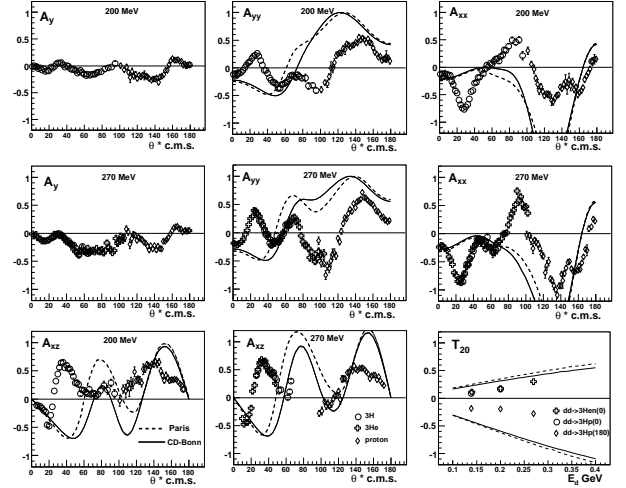
Fig. 7. The data on the analyzing powers in $d(d, {}^3\text{He})n$ and $d(d, {}^3\text{H})p$ at 270 and 200 MeV [53]. The curves are the calculation within one-nucleon-exchange approximation [33].

The measurement of the tensor analyzing power T_{20} in the $d(d, p)^3\text{H}$ and $d(d, {}^3\text{He})n$ reactions at the deuteron energies 1–2 GeV can be performed using the same experimental setup as for the ${}^3\text{He}(d, p)^4\text{He}$ reaction studies.

3.1 Polarized ${}^3\text{He}$ target

Several modifications to the existing CNS spin-exchange-type polarized ${}^3\text{He}$ target [22] have been introduced for experiment at Nuclotron-M.

A Fiber Array Packaged Laser(COHERENT FAP-79-30C-800-LB) was installed to improve the optical pumping efficiency. Small light emittance due to the introduction of the fiber provides large transmission efficiency through optical elements and good parallelness of the irradiated beam on the target cell.

Correction coils to control the magnetic field homogenity has been introduced. The coils are placed inside of larger Helmholtz coils which generate a homogeneous holding field of ~ 15 G. The purpose is to extend the area of the field homogeneity better than 10^{-3} cm^{-1} to cover the enlarged target cell size of 30 cm.

A diagnostics system to measure the ${}^3\text{He}$ density and polarization accurately has established. Target density measurement with the pressure broadening method for the Rb D_1 was introduced. By using the optical method, one can deduce the target density with high precision and high accuracy (relative error of $\sim 2\%$). New systems for the measurements of the polarization of the target using NRM

and density of the target has been manufactured, installed and tested.

The modified target is ready for the experiment at Nuclotron-M and has been used in the experiment on the polarization observables in the ^{3}He$(p, p)pX$ reaction studies at RCNP [55].

3.2 Polarized deuteron beam

To study the spin observables for the ^{3}He$(d, p)^4$He reaction new high intensity PIS [23] with the full intensity of $\sim 2 \cdot 10^{10}$ ppp is required. In this case one can measure T_{20} and $C_{y,y}$ simultaneously using polarized ^{3}He target of 30 cm thick. New source will allow to have wide number of spin states with different combination of vector and tensor polarizations. In the experiment it is planned to use the modes with the following ideal values of (p_z, p_{zz}): (0,0), (0,-2), (2/3,0) and (-1/3,+1). The polarization of the beam will be measured by the ITS polarimeter based on the asymmetry measurement of dp- elastic scattering [24, 25].

3.3 Beam parameters and setup layout

The position of the polarized ^{3}He target will be ~ 8 m downstream of the focus F3 of the Nuclotron extraction line. The results of the deuteron beam parameters measurements performed at the energies between 1000 and 2000 MeV at the focus F3 of the extraction line at Nuclotron [56] demonstrate that the beam parameters from Nuclotron are good enough to perform the experiment. However, it is necessary to modify the beam line to remove additional matter along the extraction line to reduce the multiple scattering of the initial beam.

The detection system will be placed downstream focus F5 of the VP1 beam line. Calculations for new magnetic optics have been performed [57]. The emittance of the primary beam assumed is 10-20π mm·mr, the size of the beam (2σ) at the target is about 0.5 cm both in the X and Y direction. The fields in the magnetic elements correspond to the momentum of the proton from the reaction ^{3}He$(d, p)^4$He. The primary deuteron beam and secondaries are separated by the magnet with the bending angle of $\sim$140 mr placed upstream focus F4. Optical calculations show that the size of the secondary beam in the focus F5 is 2-3 cm. The momentum and angular acceptances are $\Delta p/p = \pm 4\%$ and $\sim$3 msr ($4\sigma_{\theta_x}\sigma_{\theta_y}$), respectively. The angular acceptance can be increased in approximately 2-3 times by the use of the lenses with larger diameter downstream the target.

In the experiment it will be necessary to select protons against background deuterons with the same momentum, on the one hand, and to provide a good momentum resolution to select protons from the ^{3}He$(d, p)^4$He reaction, on the other hand.

The setup will consist of analyzing magnet, scintillation counters and drift chambers. The scintillation counter and a set of drift chambers is placed at the focus F5 upstream the analyzing magnet. The second set of the drift chambers, trigger counters and scintillation counters hodoscope are placed downstream the magnet. The size of the drift chambers placed in front of the analyzing magnet can be about 10×10 cm^2 according the calculations for magnetic optics [57].

The identification of the particles will be done by the measurements of their time-of-flight (TOF) over a baseline of about 30 m. Three scintillation counters viewed from both sides by XP2020 will be used for the trigger purpose and as the start detectors for the time-of-flight measurements. The additional set of the scintillation counters are placed in the focus F4 to provide time-of-flight measurements. The time-of-flight baseline of about 30 m is enough to separate the deuterons and protons with the same momentum up to 3.0 GeV/c.

The momentum of the particles is reconstructed via the measurements of the bending angle in the analyzing magnet. The sets of the drift chambers will be used as the tracking detectors. With the bending angle of $\sim$200 mr the momentum resolution of $\sim 0.1\%$ will be achieved.

Fast VME based DAQ system will be used for the data taking. However, in the case of large yield of deuterons this background can be suppressed partly by the second level trigger based on the measurements of the particles time-of-flight. The preparation of the time-of-flight counters [58], DAQ and HV systems [17] is in progress.

4 Polarimetry at Nuclotron-M

The spin part of *DSS* - project requires good knowledge of the deuteron beam polarization and its permanent monitoring during data taking. It crucial also to establish a polarimetry suited for a vector-tensor mixed polarized beam provided by new LHEP PIS [23].
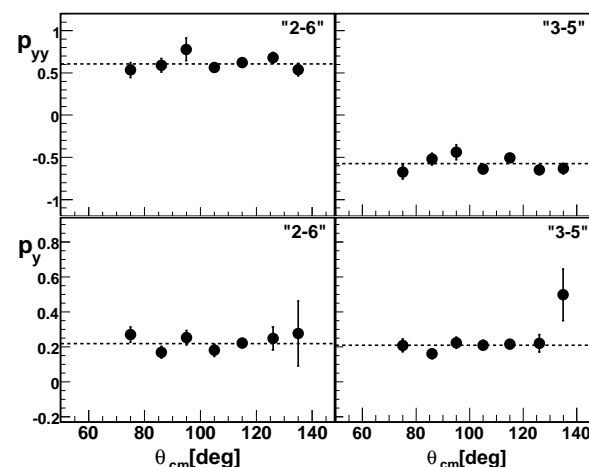

Fig. 8. Results of the beam polarization measurements for different spin modes of POLARIS [27] by ITS polarimeter at 270 MeV.

In the framework of *DSS* - project new polarimetry scheme at Nuclotron-M will be established. The basic po-

larimeter in this scheme is the polarimeter at ITS with the dp- elastic scattering at backward angles ($\theta_{cm} > 60°$) at the energies 270–2000 MeV as the analyzing reaction [16]. This polarimeter has several advantages. Firstly, both vector and tensor analyzing powers for the reaction can have large values. Therefore, such polarimeter can allow to measure both vector and tensor beam polarizations and also the spin direction. Secondly, a kinematic coincidence measurement of deuteron and proton with simple plastic scintillation counters suffices for event identification. This is mainly due to a small background event rate, compared with the forward angles. The use of this reaction as a deuteron polarimetry at 140–270 MeV at large angles has been established at RIKEN [8–10].

The first calibration data obtained at 880 MeV and 2000 MeV demonstrated the feasibility of such polarimeter [59]. The use of large amount of the scintillation counters allowed to cover wide angular range. The results on the vector and tensor beam polarizations for different spin modes of POLARIS [27] by ITS polarimeter at 270 MeV at different angles in c.m. are shown in Fig. 8. The beam polarization values were evaluated from the dp- elastic scattering asymmetries and values of the analyzing powers obtained with high precision from absolute calibration of the beam polarization at RIKEN [28]. The tensor and vector beam polarization values can be obtained with the precision better than 2%.

The ITS polarimeter will be calibrated in a wide energy range with reasonable energy step. The expected precision of the analyzing powers calibration is 2-3% at the energies below 900 MeV. The results on the analyzing powers A_y, A_{yy} and A_{xx} in dp- elastic (H_2) and quasi-elastic (CH_2) scattering at 880 MeV presented in Fig. 9 [59] demonstrate minor influence of carbon in this energy domain.
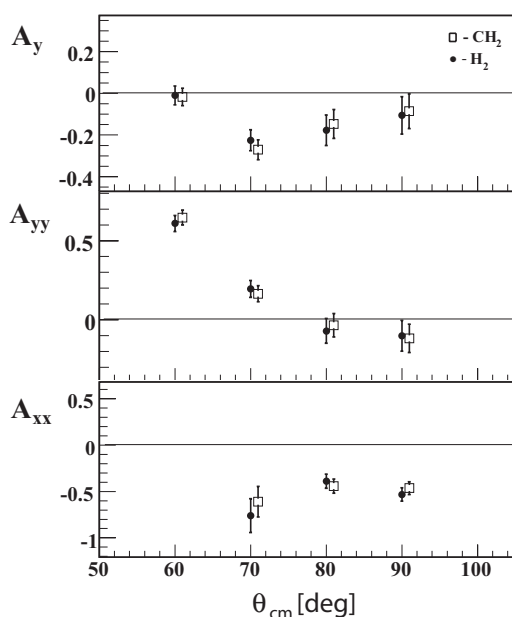
At higher energies (above 1000 MeV) the carbon content of CH_2 gives much higher contribution. However, the results on the behavior of the vector A_y and tensor A_{yy} analyzing powers for of dp- quasi-elastic scattering obtained at 2000 MeV [25] demonstrate the sizable values of these analyzing powers. This can simplify significantly the deuteron beam polarimetry at high energies. The expected precision of the analyzing powers calibration is 3-5% at the energies between 1000 and 2000 MeV.
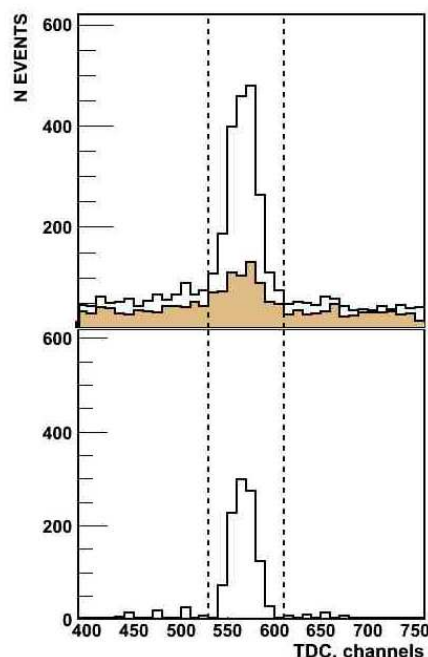
Fig. 10. Selection of the dp- elastic scattering events at θ^d_{lab}=8° and T_d =2000 MeV at extracted Nuclotron beam. The open and shadowed distributions in the upper panel are the events obtained on CH_2 and carbon targets, respactively. The results of CH_2-C subtraction are presented in the bottom panel. The dashed lines are the prompt timing windows for the final selection of the dp-elastic events.

Three different polarimeters at external Nuclotron-M beam will be calibrated with the precision 3-5% at 1600 MeV. The vector polarimeter based on quasi-elastic pp- scattering [60] and located in focus F3 is necessary for the program with polarized nucleons. Deuteron inclusive breakup polarimeter [61] with the detection of protons with the momentum $p_p = 2/3 \cdot p_d$ can be useful for the experiments where only tensor effects are studied. The use of these both polarimeters simultaneously allowed to measure both tensor and vector polarizations of the extracted beam [39]. Such tensor polarimeter will be based on the use of the magnetic spectrometer for the ^{3}He(d, p)^{4}He reaction measurements.

New high energy polarimeter based on dp- elastic scattering at forward angles, where both A_y and A_{yy} have large values [37,38], will be also located in focus F3. The dp- elastic scattering events will be detected by the

Fig. 9. Analyzing powers A_y, A_{yy} and A_{xx} in dp- elastic (H_2) and quasi-elastic (CH_2) scattering at 880 MeV [59].

kinematic coincidence of deuteron and proton with plastic scintillation counters. The final selection of useful events will be performed using amplitude and timing information. The result of the dp- elastic scattering events selection at θ_{lab}^d=8° and T_d =2000 MeV via CH_2-C subtraction of timing spectra [62] is shown in Fig. 10. The open and shadowed distributions presented in the upper panel in Fig. 10 are the events obtained on CH_2 and carbon targets, respactively, while the results of CH_2-C subtraction are presented in the bottom panel. The dashed lines are the prompt timing windows for the final selection of the dp-elastic events.

The goal of the DSS- project is to establish the polarization standard for high energy deuteron beam polarimetry at Nuclotron-M (initially based on the high accuracy dp- elastic scattering data obtained at RIKEN [28]).

5 Study of SRCs at NICA

New heavy ion and polarized particles collider NICA is planned for the energies $\sqrt{s_{NN}}$ ~4–12 GeV and up to $\sqrt{s}$ ~27 GeV for dd- and pp- collisions, respectively. The serious advantage of this facility is the availability of polarized deuterons (neutrons). The main topics of the spin studies at NICA is the spin content of nucleon, nuclear and color transparency in spin observables, polarization effects in hyperon production, single and double asymmetries in meson production, NN and light nuclei short-range spin structure [63].

Deuteron and ^{3}He(^{3}H) spin structure can be studied using two-arms magnetic spectrometer from $dd \rightarrow pX$ [39], $dd \rightarrow {}^3\text{He}n({}^3\text{H}p)$ [53], $^3\text{He}^3\text{He} \rightarrow ppX$ and other reactions. The deuteron internal structure in the $dd \rightarrow pX$ process can be probed at NICA energies up to p_T ~2–3 GeV/c, where different models predict significantly different behavior of the cross section [64]. The results of the cross section data in the $dp \rightarrow pX$ reaction calculations for laboratory frame at P_d=40 GeV/c [64] using standard [30] and covariant DWF [65] for different proton emission angles are shown in Fig. 11 and Fig. 12, respectively. For collider mode such calculations correspond to $\sqrt{s}$ ~5.3 GeV/c^2 and proton emission angles around 90° with respect to the beam direction. The results strongly deviate for the calculations based on the use of the standard and covariant DWFs [64] as well as from the constituent counting rule prediction [66,67]. The cross section data for deuteron breakup reaction at these energies are sensitive also to the problem of hidden color in nuclei via the measurement of the cross section ratio for $N(d, p\pi^+)X$ and $N(d, p)X$ processes [66].

NICA will provide the opportunity to measure tensor analyzing power A_{yy} and polarization transfer coefficient K_y^y in deuteron inclusive breakup with the proton emission at large p_T. The data on the tensor analyzing power A_{yy} obtained in the $A(d, p)X$ reaction at different values of $x_F \sim 0.61$, ~ 0.67, ~ 0.72 and ~ 0.78 and plotted as a function of the proton transverse momentum p_T are shown in Fig. 13 a), b), c) and d), respectively. The figure
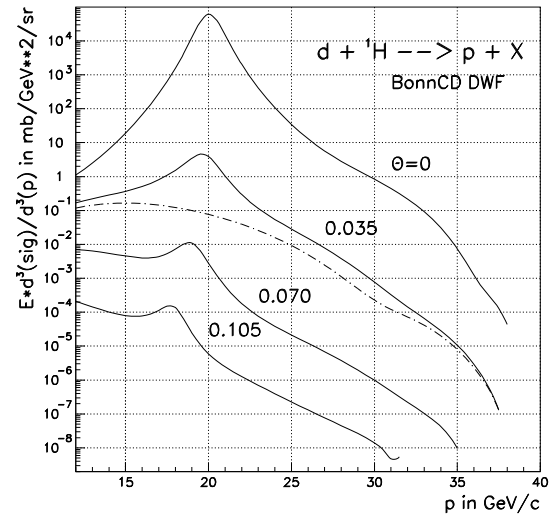

Fig. 11. The calculations for the $dp \rightarrow pX$ reaction cross section at P_d=40 GeV/c ($\sqrt{s}$ ~5.3 GeV/c^2) for different proton emission angles [64] in mr using CD-Bonn DWF [30].
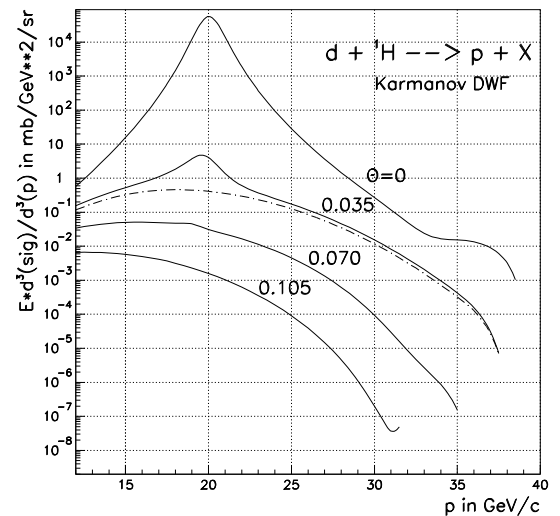

Fig. 12. The calculations for the $dp \rightarrow pX$ reaction cross section at P_d=40 GeV/c ($\sqrt{s}$ ~5.3 GeV/c^2) for different proton emission angles in mr [64] using covariant DWF [65].

is taken from ref.[39]. It is seen that the A_{yy} data for different x_F are strongly dependent of the transverse momentum of the protons, p_T. Values of A_{yy} are positive at small p_T and monotonously decrease while transverse momentum increasing for all x_F values. On the other hand, A_{yy} values change the sign at $p_T \sim 600$ MeV/c independently on x_F and demonstrate kind of negative asymptotic at large p_T. Note, that the same features are observed in the behavior of A_{yy} in dp- elastic scattering at large p_T (see Fig. 3).
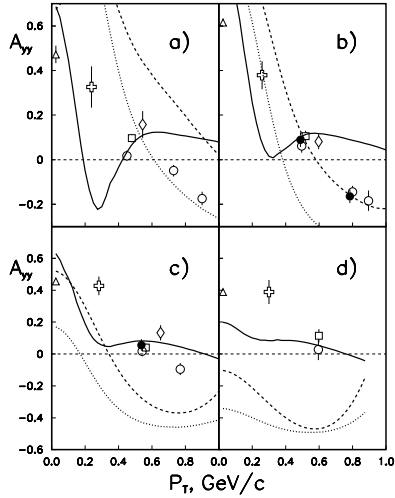
Fig. 13. A_{yy} data for deuteron inclusive breakup plotted versus proton transverse momentum p_T at four different fixed values of $x_F \sim 0.61$, 0.67, 0.72 and 0.78, are shown in a), b), c) and d) panels, respectively [39]. The dashed, dash-dotted and solid curves are the results of the calculations using standard [30,68] and covariant [65] DWFs, respectively.
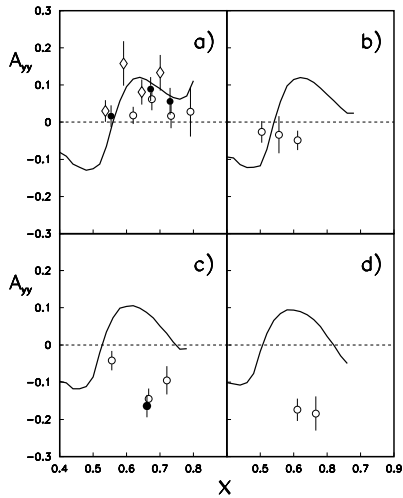
Fig. 14. A_{yy} data plotted as a function of longitudinal momentum fraction x_F obtained at fixed p_T values of ~550 MeV/c, ~700 MeV/c, ~800 MeV/c and ~900 MeV/c and shown in a), b), c) and d) panels, respectively [39]. The curves are the results of calculation using covariant DWF [65].

In Fig. 14 the A_{yy} data are plotted at different values of transverse momenta p_T as a function of x_F. The data shown in panels a), b), c) and d) correspond to the averaged values of $p_T \sim550$ MeV/c, ~700 MeV/c, ~800 MeV/c and ~900 MeV/c, respectively. The figure is taken from ref.[39]. The solid curves are the results of the calculations by using covariant DWF [65]. One can see that the A_{yy} data for different values of p_T demonstrate a weak dependence on x_F.

The data obtained at $p_T \sim550$ MeV/c are in a good agreement with the calculations by using covariant DWF [65]. At higher p_T A_{yy} data have negative values, while the theory predicts a positive sign in the range of measurement

Therefore, the A_{yy} data clearly demonstrate the dependence on two internal variables, x_F and p_T (or their combinations). However, the use of the deuteron structure function that depends on two variables [65] does not allow to describe the data. The measurements of the tensor analyzing power A_{yy} and polarization transfer coefficient K_y^y in deuteron inclusive breakup, $dd \rightarrow pX$, at $p_T \geq 1$ GeV/c at NICA is feasible and can bring new information on the spin dependence of 2N SRCs.

The collider mode gives very serious advantage to study 2N and 3N SRCs in nuclei from the $A(p, pp)X$ and $A(p, pn)X$ processes because of large coverage of the phase space for the correlated nucleon pairs in the laboratory system. Color transparency can be studied in $N(d, pp)n$ and $A(d, pp)X$ collisions [69] by the detection of two protons at large transverse momenta. These studies can be complimentary to U-70 and J-PARC scientific programs.

6 Conclusions

- The spin structure of 2N and 3N correlations can be studied at Nuclotron-M both at internal and extracted beams in the few-nucleons interaction.
- The putting into operation new PIS [23] will significantly increase the potentialities of these studies at Nuclotron-M.
- The collider mode and availability of polarized beams provide serious advantages to study 2N and 3N SRCs at NICA.

References

1. L. Frankfurt, M. Sargsian, and M. Strikman, Int.J.Mod.Phys.**A23** (2008) 2991.
2. E. Piasetzky, M. Sargsian, L. Frankfurt, M. Strikman, and J.W. Watson, Phys.Rev.Lett. **97** (2006) 162504.

3. L.L. Frankfurt, M.I. Strikman, D.B. Day, and M.M. Sargsian, Phys.Rev. **C48** (1993) 2451.
4. K.Sh. Egiyan *et al.*, Phys.Rev. **C68** (2003) 014313.
5. K.S. Egiyan *et al.*, Phys.Rev.Lett. **96** (2006) 082501.
6. L. Frankfurt, M. Sargsian, and M. Strikman, AIP Conf.Proc.**1056** (2008) 322.
7. W. Glöckle, H. Witala, D. Hüber, H. Kamada, and J. Golak, Phys.Rep. **274** (1996) 107.
8. N. Sakamoto *et al.*, Phys.Lett. **B367** (1996) 60.
9. K. Sekiguchi *et al.*, Phys.Rev. **C65** (2002) 034003.
10. K. Sekiguchi *et al.*, Phys.Rev. **C70** (2004) 014001.
11. K. Hatanaka *et al.*, Phys.Rev. **C66** (2002) 044002.
12. R. Bieber *et al.*, Phys. Rev. Lett. **84** (2000) 606.
13. K. Ermisch *et al.*, Phys. Rev. Lett. **86** (2001) 5862.
14. K. Ermisch *et al.*, Phys. Rev. **C68** (2003) 051001.
15. V.I. Kukulin *et al.*, J. Phys. G: Nucl. Part. Phys. **30** (2004) 287.
16. T. Uesaka *et al.*, Phys.Part.Nucl.Lett **3** (2006) 305.
17. S.M. Piyadin *et al.*, submitted to Eur.Phys.J. ST (2009).
18. A.I. Malakhov *et al.*, Nucl.Instr.Meth. in Phys.Res. **A440** (2000) 320.
19. T. Uesaka *et al.*, Phys.Lett. **B467** (1999) 199.
20. H. Kamada *et al.*, Prog.Theor.Phys. **104** (2000) 703.
21. T. Uesaka *et al.*, Phys. Lett. **B533** (2002) 1.
22. T. Uesaka *et al.*, Nucl.Instr. and Meth. in Phys.Res. **A402** (1998) 212.
23. V.V. Fimushkin *et al.*, Eur.Phys.J. ST **162** (2008) 275.
24. K. Suda *et al.*, AIP Conf.Proc. **915** (2007) 920; AIP Conf.Proc. **1011** (2008) 241.
25. P.K. Kurilkin *et al.*, Eur.Phys.J. ST **162** (2008) 137; Int.J.Mod.Phys. **A24** (2009) 530.
26. Yu.V. Gurchin *et al.*, Phys.Part.Nucl.Lett. **4** (2007) 263.
27. N.G. Anishchenko *et al.*, AIP Conf.Proc. **95** (1983) 445.
28. K. Suda *et al.*, Nucl.Instr.Meth. in Phys.Res. **A572** (2007) 745.
29. H. Witala, private communication.
30. R. Machleidt, Phys. Rev.C **63** (2001) 024001.
31. N.B. Ladygina, Phys.Atom.Nucl. **71** (2008) 2039; N.B. Ladygina, e-Print: arXiv:0805.3021[nucl-th].
32. M.A. Shikhalev, Phys.Atom.Nucl. **72** (2009) 588.
33. N.B. Ladygina, Eur.Phys.J. **A42** (2009) 91.
34. N.E. Booth *et al.*, Phys.Rev. **D4** (1971) 1261.
35. J.C. Alder *et al.*, Phys.Rev. **C6** (1972) 2010.
36. M. Garson *et al.*, Nucl.Phys. **A458** (1986) 287.
37. M. Bleszynski *et al.*, Phys.Lett. **B87** (1979) 178; ibid. **B106** (1981) 42; M. Haji-Saied *et al.*, Phys.Rev. **C36** (1987) 2010.
38. V. Ghazikhanian *et al.*, Phys.Rev. **C43** (1987) 1532.
39. V.P. Ladygin *et al.*, Phys.Lett. **B629** (2005) 60; L.S. Azhgirey *et al.*, Phys.Atom.Nucl. **71** (2008) 279.
40. A.D. Krisch, Eur.Phys.J. **A31** (2007) 423.
41. S. Kistryn *et al.*, Phys.ReV. **C68** (2003) 054004; ibid. **C72** (2005) 044006.
42. K. Sekiguchi *et al.*, Phys.ReV. **C79** (2009) 054008.
43. M. Eslami-Kalantari *et al.*, Mod.Phys.Lett.**A24** (2009) 839.
44. E. Stephan *et al.*, Int.J.Mod.Phys.**A24** (2009) 515.
45. H. Witala, J. Golak, and R. Skibinski, Phys.Lett.**B634** (2006) 374.
46. H. Witala *et al.*, Mod.Phys.Lett.**A24** (2009) 871.
47. V.P. Ladygin and S. Nedev, Part. and Nucl.Lett. **2[111]-2002** (2002) 13.
48. V. Punjabi *et al.*, Phys.Lett. **B350** (1995) 178.
49. L.S. Azhgirey *et al.*, Phys.Lett. **B391** (1997) 22.
50. D. Abbott *et al.*, Phys.Rev.Lett. **84** (2000) 5053.
51. V. Punjabi *et al.*, Phys.Rev. **C39** (1989) 608.
52. L.S. Azhgirey *et al.*, Phys.Lett. **B387** (1996) 37.
53. A.K. Kurilkin *et al.*, Eur.Phys.J. ST **162** (2008) 133; V.P. Ladygin *et al.*, Phys.Lett. **B589** (2004) 47; M. Janek *et al.*, Eur.Phys.J. **A33** (2007) 39.
54. N.B. Ladygina, private communication.
55. Y. Shimizu *et al.*, *Proc. of the 19-th Few Body Conference* (Bonn, Germany, 2009), to be published.
56. M. Janek *et al.*, JINR Preprint **P1-2007-171**, Dubna (2007).
57. P.A. Rukoyatkin, private communications.
58. A.A. Terekhin *et al.*, to be published in Vestnik BGU (2009).
59. T. Uesaka *et al.*, CNS Report **79**, Tokyo (2008).
60. L.S. Azhgirey *et al.*, Instr. and Exp.Tech. **40** (1997) 43; Nucl.Instr.Meth. in Phys.Res. **A497** (2003) 340.
61. L.S. Zolin *et al.*, JINR Rapid Comm. **2[88]-98** (1998) 27; Yu.K. Pilipenko *et al.*, AIP Conf. Proc. **570** (2001) 801.
62. Yu.V. Gurchin *et al.*, submitted to Phys.Part.Nucl.Lett. (2009).
63. V.P. Ladygin *et al.*, AIP Conf.Proc. **1056** (2008) 420.
64. L.S. Azhgirey *et al.*, Phys.Part.Nucl.Lett. **4** (2007) 497.
65. V.A. Karmanov and A.V. Smirnov, Nucl.Phys. **A546** (1992) 691; ibid. **A575** (1994) 520; J. Carbonell and V.A. Karmanov, Nucl.Phys. **A581** (1995) 625; ibid. **589** (1995) 713; J. Carbonell, B. Desplanques, V.A. Karmanov, and J.F. Mathiot, Phys.Rep. **300** (1998) 125.
66. S.J. Brodsky and G.R. Farrar, Phys.Rev.Lett. **31** (1973) 1153; Phys.Rev. **D11** (1975) 1309; G.P. Lepage and S.J. Brodsky, Phys.Rev. **D22** (1980) 2157.
67. V.A. Matveev, R.M. Muradyan, and A.N. Tavkhelidze, Lett. Nuovo Cim. **7** (1973) 719.
68. M. Lacombe, B. Loiseau, R. Vinh Mau, J. Cote, P. Pires, and R. de Tourreil, Phys.Lett. B **101** (1981) 139.
69. L.L. Frankfurt, E. Piasetzky, M.M. Sargsian, and M.I. Strikman, Phys.Rev. **C56** (1997) 2752.